Korean J. Chem. Eng., 34(1), 179-188 (2017)
DOI: 10.1007/s11814-016-0217-0

pISSN: 0256-1115
eISSN: 1975-7220

Thermodynamics and kinetics study of defluoridation using Ca-SiO_2-TiO_2 as adsorbent: Column studies and statistical approach

Swapnila Roy†, Papita Das, and Shubhalakshmi Sengupta

Department of Chemical Engineering, Jadavpur University, 188, Raja Sc. Mullick Rd., Kolkata-700032, India
(*Received 8 April 2016 • accepted 30 July 2016*)

Abstract−Fluoride contamination of water is a potential health and environmental hazard worldwide. This study focuses on defluoridation efficiency in aqueous system by novel adsorbents, i.e., calcium impregnated silica (Ca-SiO_2) and calcium impregnated silica combined with titanium dioxide (Ca-SiO_2-TiO_2). Comparative batch study was carried out using both adsorbents Ca-SiO_2 and Ca-SiO_2-TiO_2 for fluoride removal efficiency in different experimental conditions where it was observed that chemically modified Ca-SiO_2-TiO_2 acted as a better adsorbent for defluoridation than Ca-SiO_2. Thus, further batch isotherm and kinetics studies were performed using Ca-SiO_2-TiO_2. The phenomenon of fluoride ion uptake is realized by Langmuir and Freundlich isotherm model. Langmuir isotherm shows satisfactory fit to the experimental data. The rate of adsorption shows that the pseudo-second-order rate fitted the adsorption kinetics better than the pseudo-first-order rate equation. The mechanism of adsorption process was illustrated by calculating Gibbs free energy, enthalpy and entropy from thermodynamic studies. To further confirm the applicability of the adsorbent, a fixed bed study was carried out in column mode. Thomas and bed-depth-service-time (BDST) model were well-fitted to the experimental results. The optimal operating conditions of defluoridation were found by using response surface methodology (RSM) with the help of Design Expert Software. The maximum percentage of fluoride removal was 92.41% in case of calcium impregnated silica combined with titanium dioxide (Ca-SiO_2-TiO_2). Thus, it may be concluded that chemically synthesized Ca-SiO_2-TiO_2 could be used as an environmentally and economically safe adsorbent for defluoridation of waste water.

Keywords: Defluoridation, Ca-SiO_2-TiO_2, Response Surface Methodology, Fixed-bed Adsorption Study, Langmuir Isotherm Model

INTRODUCTION

Fluorine is a naturally available element which does not exist in nature in its elemental form but as fluorides in various minerals (fluorspar, cryolite and flourapatite) due to its high reactivity [1]. Inorganic fluoride compounds are used in various ceramic and nano-technology based industries. Compounds like fluorosilicic acid and sodium hexafluorosilicate are used in water fluoridation. In several studies, it was revealed that daily fluoride uptake widely varied according to the various sources of exposure. Increased uptake of fluoride in drinking water results in fluoride absorption in the gastrointestinal tract from where it is transported through blood with subsequent accumulation in teeth, bones and skeletal tissues causing serious health hazards like skeletal fluorosis at a consumption level of 3-6 mg/*l* of fluoride in water [2]. Statistically significant trend of increased incidences of osteosarcomas with an increase in fluoride exposure in animals has also been also reported. Thyroid activity is also affected by fluoride exposure. These toxicological effects [3] of fluoride on living organisms and human health requires an urgent need to develop an effective method for the removal of excess fluoride from drinking water.

†To whom correspondence should be addressed.
E-mail: swapnilaroy@gmail.com

Different types of methods have been used for defluoridation in water such as adsorption, ion exchange, precipitation, electrolysis, donnan dialysis, and electrodialysis [4,5]. Adsorption is the cheapest and most extensively used method for defluoridation [6,7]. Recent research studies revealed that several low-cost materials were used for defluoridation such as bentonite, kaolinitic clay, agricultural waste products, fly ash, carbon slurry, bone char, and activated carbon [8-10].

The defluoridation by adsorption processes could be elucidated effectively by the application of statistical experimental design techniques, which results in improved product yields, reduced variation in process parameters, closer confirmation of the output response to nominal and target.

In many research studies, RSM (Response surface methodology) was used to estimate the relationship between a set of experimental factors and calculated results [11]. Usually, three level complete factorial designs (Box-Behnken model) was used to estimate the effects of major operating variables on fluoride adsorption and to find the combination of variables resulting in maximum de-fluoridation efficiency [12,13]. This design was applied using Design Expert Software Version 7.6.1 (Stat Ease, USA). In this study, the combined effects of adsorbent dose, contact time and temperature on fluoride removal from aqueous medium by Ca-SiO_2-TiO_2 were investigated using CCD (Central composite design) in RSM. The RSM [14-17] has graphic representation of a response surface

method in three dimensions. Actually, this is four-dimensional space, which is represented since the three factors are in 3-dimensional space and the response is the 4th dimension.

Thus, the present study aims to highlight defluoridation [18] by novel adsorbents: calcium impregnated silica (Ca-SiO_2) and calcium impregnated silica combined with titanium dioxide (Ca-SiO_2-TiO_2). Various process parameters such as effect of adsorbent dose, contact time, reaction temperature were experimented to study the effect of these parameters on the removal efficiency. The adsorption isotherm [19] and adsorption capacity of Ca-SiO_2-TiO_2 in batch studies and fixed-bed adsorption studies [20] were also investigated along with analysis by isotherm kinetics. Statistically, the optimized condition was achieved by using CCD in RSM.

EXPERIMENTAL

1. Materials

25% aqueous solution of calcium chloride ($CaCl_2 \cdot 2H_2O$) [Merck, Germany], Silica (SiO_2) [Merck, Germany], Titanium dioxide (TiO_2) [Merck, Germany], Sodium Fluoride [Merck, Germany] were used for preparation of adsorbents and stock fluoride solution. All the chemicals were of reagent grade and ultrapure distilled water were used in all the preparations.

2. Preparation of Adsorbents

2-1. Ca-SiO_2

Silica(SiO_2) was the precursor for the preparation of calcium impregnated silica (Ca-SiO_2). A known quantity of dried and grinded silica (SiO_2) was mixed with 25% $CaCl_2$ aqueous solution (w/v) in the specific ratio (5 : 12). The obtained slurry was rinsed thoroughly with distilled water several times. The washed slurry was then dried and finally calcium impregnated silica was collected which was kept in a muffle furnace at 500 °C for 6 hrs. The final product was cooled and taken out after 30 minutes and kept in a desiccator for further study.

2-2. Ca-SiO_2-TiO_2

In this case similarly Silica (SiO_2) and Titanium dioxide (TiO_2) [21] were the precursor for the preparation of calcium impregnated silica combined with titanium dioxide (Ca-SiO_2-TiO_2). The mixture of 5 g dried and ground silica (SiO_2) and 5 g titanium dioxide (TiO_2) were added to 24 mL of 25% $CaCl_2$ aqueous solution (w/v). Then the mixture was stirred for 30 minutes. After that the obtained slurry was washed several times with distilled water. Then it was kept in a muffle furnace at 500 °C for 6 hrs. The final product was cooled and taken out after 30 minutes and kept in a desiccator for further study.

3. Characterization of Ca-SiO_2 and Ca-SiO_2-TiO_2

3-1. XRD (X-ray Diffraction) Analysis

X-ray diffraction analysis of the adsorbent involved using X-ray diffractometer equipment (Bruker, D8 Advance, Germany) with a Cu Kα radiation at an accelerating voltage 40 kV and emission current 30 mA in the range of diffraction angle 2θ=10-80°. The XRD pattern of Ca-SiO_2-TiO_2 as prepared is represented in Fig. 1(a).

3-2. SEM (Scanning Electron Micrograph)

The Scanning Electron Microscope (SEM) image (JEOL-JSM-6360, Jeol, Japan) of Ca-SiO_2-TiO_2 at magnification 1000X were obtained, depicted in Fig. 1(b).

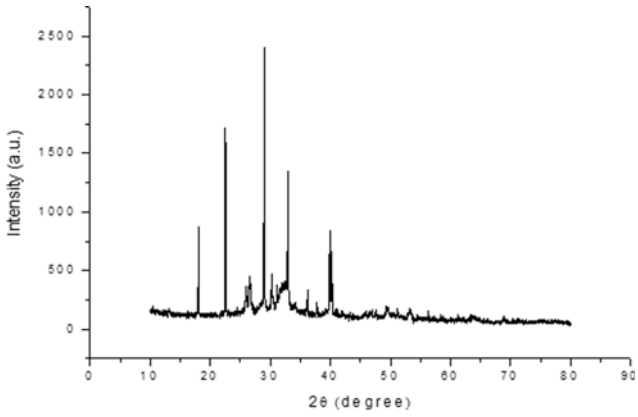

(a)

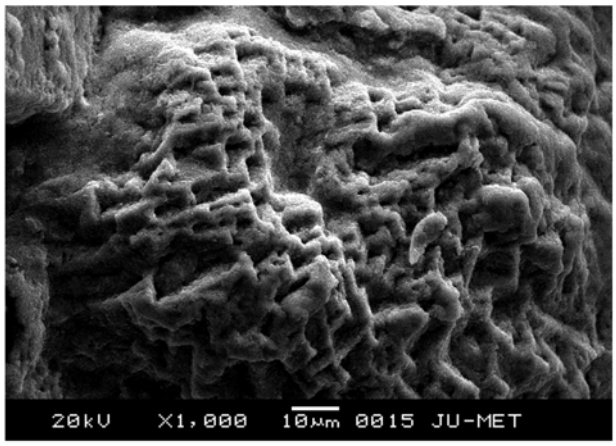

(b)

Fig. 1. (a) XRD of Ca-SiO_2-TiO_2, (b) SEM of Ca-SiO_2-TiO_2 at 1000×.

4. Batch Setup

For batch experiments, 100 mL fluoride solutions of concentration 50 mgL^{-1} were taken in 250 mL PTFE (Polytetrafluoroethylene) conical flasks. These two adsorbents were added in the required quantity (0.5 g, 0.75 g, 1 g, 1.5 g) to 100 mL fluoride solution within the range of temperature (303-353 K) following the range of contact time (10-100 min) to achieve optimized condition for adsorbent dose (g/100 mL), contact time (min) and temperature (K).

Experiments were conducted in a temperature controlled incubator shaker (INNOVA 4430, New Brunswick Scientific, Canada). Then the flasks were agitated at 150 rpm in an incubator shaker at different temperatures. After shaking for particular time intervals, those samples were collected from the flasks for analysis of residual fluoride concentration in the solution. The dissolved fluoride in each conical flask was estimated by ion-meter (Thermo Scientific Orion ion-meter, USA). The effects of contact time(10-100 min) adsorbent dose (0.5-1.5 g/100 mL) and temperature (303-353 K) were evaluated during the batch studies.

5. Isotherm, Kinetics and Thermodynamics Studies

5-1. Adsorption Isotherm

The isotherm models, Langmuir and Freundlich isotherms, were investigated by using Ca-SiO_2-TiO_2 for defluoridation in water. The interaction between fluoride ions and adsorbents can be better explained by these isotherm models.

• **Langmuir Isotherm**

The linear form of Langmuir model [22] is given by the following equation:

$$\frac{C_e}{Q_e}=\frac{1}{Q_0 b}+\frac{C_e}{Q_0} \quad (1)$$

where C_e is the residual fluoride concentration at equilibrium, Q_e is the fluoride concentration adsorbed on the sorbent at equilibrium, Q_o denotes maximum fluoride concentration and b is the Langmuir constant.

• **Freundlich isotherm**

The Freundlich isotherm [23] constants are estimated using the following equation:

$$\mathrm{Ln}Q_e=\mathrm{Ln}K_F+\left(\frac{1}{n}\right)\mathrm{Ln}C_e \quad (2)$$

where Q_e is the amount of fluoride adsorbed at equilibrium, and K_F and n are Freundlich

Constants denotes adsorption capacity and adsorption intensity respectively

5-2. Adsorption Kinetics

The adsorption process is carried out at various temperatures to determine the optimum temperature for maximum adsorption efficiency and for obtaining the reaction rate constant activation energy. 100 mL of fluoride solution of concentration 50 mg/L was taken in PTFE conical flask and 1 gm adsorbent is added to it. Then this mixture was agitated at 150 rpm for 1 hour. From this experiment kinetic rate constant at different temperatures is estimated.

• **Pseudo first order kinetics**

The rate constant is estimated using the following equation:

$$\frac{dq_t}{dt}=k_1(q_e-q_t) \quad (3)$$

where, q_e=fluoride adsorbed at equilibrium/unit weight of adsorbent (mg/g), q_t is the amount of fluoride adsorbed at any instant (mg/g) and k_1 is the rate constant (min^{-1}).

Integrating at these conditions as t=0 and q_t=0 to t=t and q_t=q_t, the final equation is written as given below:

$$\mathrm{Log}(q_e-q_t)=\log q_e-\frac{k_1 t}{2.303} \quad (4)$$

• **Pseudo second order kinetics**

The model equation is described as follows:

$$\frac{t}{q_t}=\frac{1}{k_2 q_e 2}+1/q_e(t) \quad (5)$$

where k_2 denotes the pseudo-second-order rate constant of adsorption (g mg^{-1} min^{-1}) and q_e and q_t are the amounts of fluoride adsorbed (mg/g) at equilibrium and at time t respectively.

• **Activation energy**

From the obtained the rate constant, activation energy of the adsorption of fluoride is estimated using Arrhenius Eq. (6) as follows:

$$\ln k_2=\ln A_0-\frac{E_a}{RT} \quad (6)$$

where E_a=activation energy (kJ mol^{-1}); R=gas constant (8.314 J mol^{-1} K^{-1}); and A_0=Arrhenius constant.

5-3. Adsorption Thermodynamics

The adsorption thermodynamic parameters of fluoride are estimated using the following formulas:

$$K_c=\frac{C_a}{C_e} \quad (7)$$

where, K_c=coefficient of distribution for the adsorption; C_a=fluoride adsorbed per unit mass of the adsorbent (mg L^{-1}); C_e=equilibrium concentration of adsorbate in aqueous phase (mg L^{-1}).

$$\Delta G_0=-RT\ln K_c \quad (8)$$

where, G_0 (kJ mol^{-1})=change of Gibb's free energy; R=universal gas constant; and T=absolute temperature (K); and

$$\ln K_c=\frac{\Delta S_0}{R}-\frac{\Delta H_0}{RT} \quad (9)$$

where ΔH_0 (kJ mol^{-1})=change of enthalpy; ΔS_0 (J mol^{-1} K^{-1})=change of entropy.

6. Fixed-bed Adsorption Studies

Continuous flow adsorption [24] experiments were carried out in a PTFE (Polytetrafluoroethylene) column (2.5 cm internal diameter and 20 cm height). A known quantity of Ca-SiO_2-TiO_2 was packed into that column to yield the desired bed height. Glass wool was attached at the bottom of the column to support the adsorbent bed and to make a good liquid distribution inside the column. 50 mg l^{-1} fluoride solution was pumped downward through the column by a peristaltic pump. All the experiments were at room temperature. Samples were collected at the outlet of the column at fixed time intervals and the concentration of fluoride in the effluent was analyzed using an ion meter (Thermo Scientific, Orion). The experiment was stopped when the effluent fluoride concentration was equal to the initial concentration.

6-1. Modeling of Fixed Bed Column Reactor

In this study, the bed-depth-service-time (BDST) model and Thomas model were well fitted to the dynamic flow experimental data of fluoride adsorption in order to determine the characteristic parameters of the column.

$$\text{BDST: } \frac{N_0}{C_0 F}Z-\frac{1}{K_a C_0}\ln\left(\frac{C_0}{C_t}-1\right) \quad (10)$$

$$\text{Thomas: } \ln\left(\frac{C_0}{C_t}-1\right)=\frac{k_{Th} q_0 m}{F}-k_{Th} C_0 t_e \quad (11)$$

where N_0 is the maximum volumetric sorption capacity (mg L^{-1}), Z is the bed height (cm), C_0 is the initial fluoride concentration (mg L^{-1}), C_t is the concentration of fluoride at time t (mg L^{-1}), u is the flow rate (mL min^{-1}), K_a is adsorption rate constant (L mg^{-1} min^{-1}), k_{Th} is the Thomas rate constant (mL mg^{-1} min^{-1}), q_0 is the equilibrium adsorbate uptake (mg g^{-1}), m is the mass of the adsorbent in the column (g), F is the volumetric flow rate (mL min^{-1}) and t_e is the bed exhaustion time (min).

7. Response Surface Methodology for Optimization of Adsorption Parameters

The determination of optimum conditions [25] for fluoride adsorption by Ca-SiO_2-TiO_2 depends on the three process variables:

Table 1. Thermodynamic parameters for the adsorption of fluoride onto Ca-SiO_2-TiO_2

Serial no.	T, K	ΔG, kJ/mol	ΔH, kJ/mol	ΔS, J mol^{-1} K^{-1}
1	300	−9.73		
2	308	−11.45		
3	320	−13.87	59.48	249.23
4	333	−14.38		
5	343	−12.61		

adsorbent dose, temperature and contact time of the solution. The experimental ranges along with the levels of variables are given in Table 1. The percent removal of fluoride is the response of the system. Statistically, the prediction of the optimum condition is obtained following the quadratic equation model given below (Eq. (12)).

$$Y = \beta_0 + \Sigma_{i=1}^{k}\beta_i x_i + \Sigma_{i=1}^{k}\beta_{ii} x_{i2} + \Sigma_{i=1}\Sigma_{j=i+1}\beta_{ij} x_i x_j + \varepsilon \quad (12)$$

Here, Y=response (i.e., dependent variable), β_0=constant coefficient, β_i=β_{ii}=β_{ij}=coefficients of linear, quadratic and interaction effect, x_i and x_j=factors (independent variables).

And ε=error.

Percentage of fluoride removal efficiency is calculated with a standard RSM design (CCD) and 20 experiments were carried out. The percent removal (%) of fluoride is determined by using the following Eq. (11):

$$R(\%) = \frac{C_i - C_0}{C_i} \times 100 \quad (13)$$

where C_i is the initial fluoride concentration (mg L^{-1}) and C_0 is the final fluoride concentration in solution (mg L^{-1}).

Design Expert Version 9.1.6 (Stat Ease, USA) was applied for graphical analysis of the experimentally obtained data. The optimum values of the independent variables were obtained by solving the regression equation and by analyzing the contour plots. The coefficient of correlation and the quadratic model [26] equation was used to predict the interaction effect of different factors within the specified range, which can be described mathematically.

8. Statistical Analysis

To maintain quality assurance, the precision, accuracy, repeatability and reproducibility of the obtained experimental data, all experiments were conducted twice. Data were analyzed and mean values and standard deviation (SD) obtained with Design Expert Version 9.1.6 (Stat Ease, USA). The three process parameters such as contact time (min), temperature (K) and adsorbent dose (g) were utilized for experimental study of de-fluoridation in response surface methodology (RSM).The interaction effect of process variables was evaluated by conducting 20 experiments using central composite design (CCD).

RESULTS AND DISCUSSION

1. Characterization of Ca-SiO_2-TiO_2

Fig. 1(a) shows the XRD pattern of Ca-SiO_2-TiO_2, which represents powder and thin film type composition. As the sample was heated at 500 °C for 6 hrs, the most intense peaks were at 2θ=

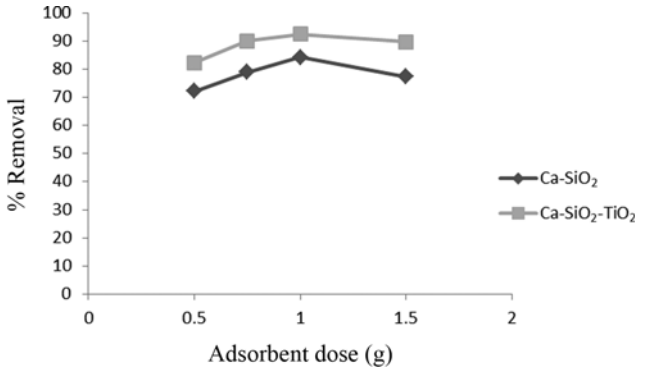

Fig. 2. Effect of adsorbent dose on removal of fluoride by Ca-SiO_2 and Ca-SiO_2-TiO_2 (experimental conditions: C_0=50 mg L^{-1}, agitation speed=200 rpm, T=333 K, contact time: 70 min).

26.4° and 26.5° which may be assigned to the characteristic peak of crystal structure. As atomic radii of Si are smaller than Ti, TiO_2 particle experiences contraction and crystal growth is retarded due to Si atom. From the XRD pattern it can be inferred that doping of SiO_2 with TiO_2 matrix with $CaCl_2$ leads to amorphous oxides.

Fig. 1(b) again represents powder and thin film surface formed due to calcination of Ca- SiO_2-TiO_2 at 500 °C for 6 hrs. It is looking like agglomerate type particles. There are some bigger particles, surrounded by smaller particles. Chemically, Ca-O-Ti-O-Si bond may be formed. The phenomena can be called the suppressive effect of SiO_2 on crystal growth of TiO_2.

2. Continuous Batch Studies

2-1. Effect of Adsorbent Dose

From the batch experimental study, it was observed (Fig. 2) that chemically modified Ca-SiO_2-TiO_2 acted as a better adsorbent for defluoridation than Ca-SiO_2. Within the experimental range of adsorbent dose in between 0.1 g-1.5 g/100 mL percent removal of fluoride gradually increases with increasing adsorbent dose, then decreases. The adsorbent dose in the range of 0.1-1.0 g/100 mL, defluoridation efficiency increases because of the number of ions increases on the adsorbent surface in both cases due to the attraction force of adsorbate ions with the adsorbent dose higher than 1.0 g/100 mL, shows decrease in removal on the adsorbent surface because surface of adsorbent reached the saturation point by fluoride ions, hence fluoride ions are further not adsorbed on adsorbent surface due to repulsive force.

It can be explained that due to availability of adsorption sites on the sorbent surface, the defluoridation efficiency increases. But after the equilibrium fluoride adsorption, decrease in defluoridation efficiency with increasing adsorbent dosage (above 1.0 g/100 mL).

2-2. Effect of Contact Time

Comparing above two plots (Fig. 3) it is seen that Ca-SiO_2-TiO_2 is a much better adsorbent than Ca-SiO_2 for defluoridation in water. It is observed from the experimental study that on increasing the contact time at particular temperature, defluoridation efficiency increases in both cases. As the contact time increases, greater are the number of fluoride ions attached on the adsorbent surface. It can be explained that accumulation of fluoride ions on adsorbent surface increases because of attraction force in between adsorbent surface and fluoride ion, consequently increasing the percent of fluo-

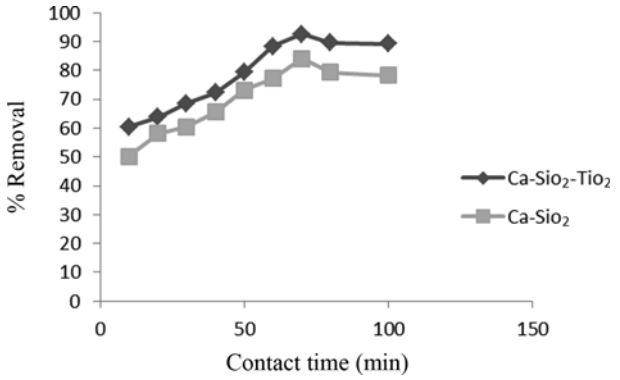

Fig. 3. Effect of contact time on removal of fluoride by Ca-SiO_2 and Ca-SiO_2-TiO_2 (experimental conditions: C_0=50 mg L^{-1}, agitation speed=200 rpm, T=333 K, adsorbent dose=1.0 g/100 ml).

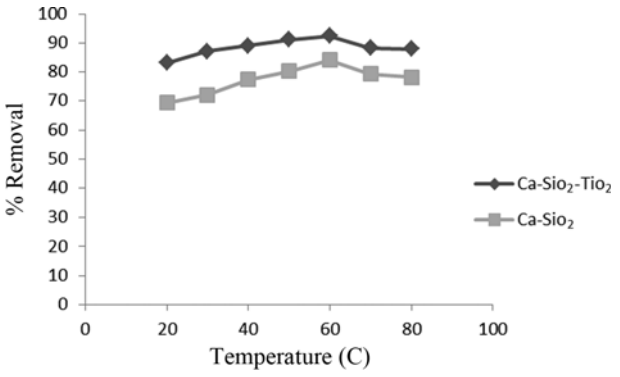

Fig. 4. Effect of temperature on removal of fluoride by Ca-SiO_2 and Ca-SiO_2-TiO_2 (experimental conditions: C_0=50 mg L^{-1}, agitation speed=200 rpm, adsorbent dose=1.0 g/100 ml, contact time: 70 min).

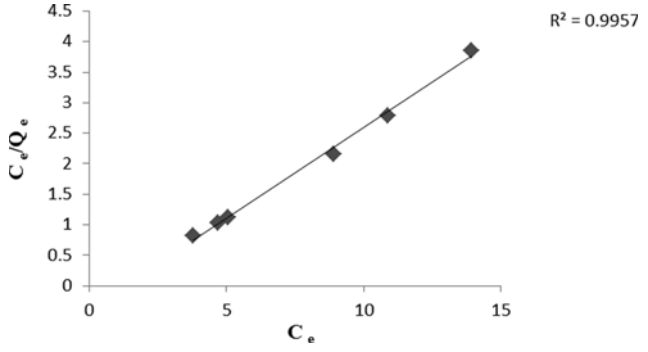

Fig. 5. Langmuir Adsorption Isotherm plots of defluoridation onto Ca-SiO_2-TiO_2 (experimental conditions: C_0=50 mg L^{-1}, agitation speed=200 rpm, T=333 K).

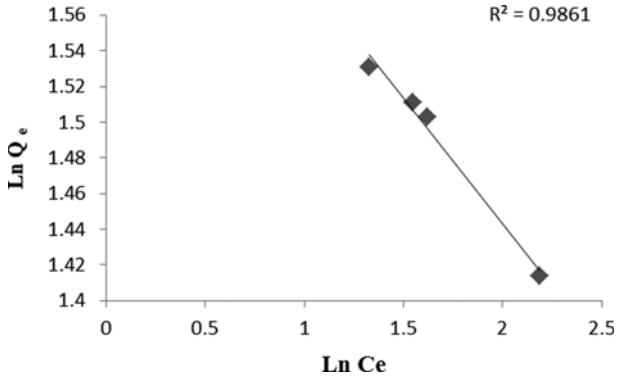

Fig. 6. Freundlich adsorption Isotherm plots of defluoridation onto Ca-SiO_2-TiO_2 (experimental conditions: C_0=50 mg L^{-1}, agitation speed=200 rpm, T=333 K).

ride removal in solution. But after certain point (70 min), defluoridation efficiency decreases as shown in the curve. This happened because the maximum number of the fluoride ions were attached on adsorbent surface when reaction time was 70 minutes. There is no significant increase after that point (70 min). So the optimized contact time is 70 min for further experimental studies. So the saturation point achieved at 70 min due to non-availability of active site for fluoride adsorption.

2-3. Effect of Temperature

It is illustrated in the experimental study (Fig. 4) that with increasing temperature, the percent removal of fluoride first increases from 300 K to 320 K. After 320 K, defluoridation efficiency decreases following the adsorption process, increasing the number of adsorbate ions (fluoride) accumulate on adsorbent surface, the attractive force in between fluoride ions and adsorbent surface (Ca-SiO_2-TiO_2 and Ca-SiO_2) increases. But as temperature increases beyond 333 K, as charge density of fluoride ions increases, the repulsive force increases between adsorbate and adsorbent surface, and consequently, the defluoridation efficiency gradually increases with increasing temperature (up to 333 K), then decreases. The mechanism of adsorption of fluoride species by the adsorbents depends upon the charges present on both adsorbent surface and adsorbate at given reaction conditions. From the experimental study it is proved that the chemically synthesized Ca-SiO_2-TiO_2 is more efficient in removal of fluoride than Ca-SiO_2.

3. Thermodynamics and Kinetics Study of Batch Experiments

3-1. Effect of Adsorption Isotherms

A graph between log Q_e and log C_e and between C_e and C_e/Q_e was plotted to obtain Langmuir and Freundlich adsorption isotherms, respectively (Fig. 5 and Fig. 6). Both Langmuir and Freundlich adsorption isotherms yield a straight line with R^2 values of 0.9957 and 0.9861, respectively, confirming the validity of both the isotherms and hence declaring the suitability of Ca-SiO_2-TiO_2 for the adsorption of fluoride ions from the solution. Comparisons between R^2 values between these isotherms show that the adsorption of fluoride has a good compliance with Langmuir adsorption model (R^2=0.9957 versus 0.986), which indicates the priority for the formation of monolayer on Ca-SiO_2-TiO_2 by fluoride species. Based on Eqs. (1) and (2) and equation curve on Fig. 5 and Fig. 6, respectively, the values of K_F, n, q_m and b were calculated and found to be 0.942, 3.02, 1.859 μg/g and 0.862 L/μg, respectively.

3-2. Effect of Adsorption Kinetics and Temperature

The linear plots of t/q_t vs t are shown in Fig. 7. At 333 K, the rate constant is 0.21 g mg^{-1} min^{-1} and the initial adsorption rate is 4.45 mg g^{-1} min^{-1}. As a consequence, from experimentally obtained results, it is proved that as temperature increased from 303 to

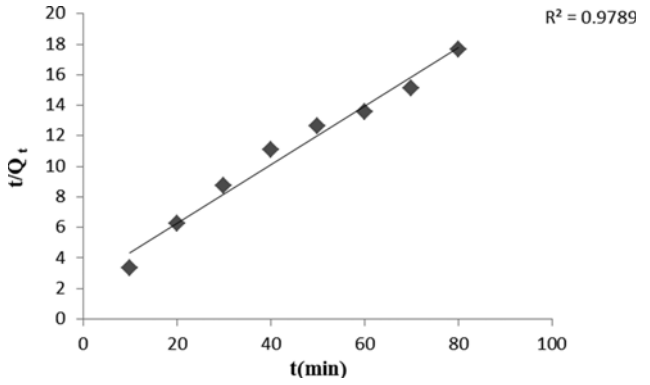

Fig. 7. Pseudo second order kinetic model for adsorption of fluoride onto Ca-SiO_2-TiO_2 (experimental conditions: C_0=50 mg L^{-1}, agitation speed=200 rpm, T=333 K).

333 K, the amount of fluoride adsorbed increased. This phenomenon occurred due to rise in the mobility of fluoride ions with temperature, and so, the adsorption capacity also increased with a rise in temperature.

From the pseudo-second-order rate constant k_2 at different temperatures, the activation energy E_a is estimated using the Arrhenius energy equation (Eq. (3)). The slope calculated from Arrhenius equation was 41.84 kJ/mol. The activation energy is greater than calculated value of Arrhenius energy.

From the batch experiment studies, it is observed that as time increases, the efficiency of the reduction of fluoride increases as well as the adsorption capacity, and after a certain time 92.45% removal of fluoride is obtained. At 333 K (Fig. 7) t/q_t vs t plot is showing a linear plot with regression coefficient 0.9789. At 333 K, the rate constant is 0.223 g mg^{-1} min^{-1} and the initial adsorption rate was 4.45 mg g^{-1} min^{-1}. This phenomenon indicates that calcium impregnated silica combined with TiO_2 can be effectively used for fluoride adsorption in batch studies.

3-3. Thermodynamic Parameters

From the experimental data following Eqs. (7)-(9) it represents that the negative value of ΔG^0 increases with increasing in the temperature (up to 333 K), which implies that the adsorption is thermodynamically feasible and the positive values of ΔH^0 support the endothermic nature of the reaction due to consuming energy from the reaction system. The values of ΔH^0 and, ΔS^0 are estimated from the slopes and intercept of the plot $\ln K_c$ vs. (1/T) (Fig. not given), and the values are listed in Table 2. It is observed that the negative value of ΔG^0 at all temperatures represents that the fluoride adsorption reaction is spontaneous. In this case ΔG^0 decreases up to 333 K, and after that it increases, which indicates that the adsorption reaction is feasible up to 333 K. As a consequence, the randomness in between fluoride ion and Ca-SiO_2-TiO_2 surface is increased. As the reaction is endothermic, it is expected that the adsorption capacity of fluoride ions by Ca-SiO_2-TiO_2 is increasing with temperature. But after 333 K, the reverse reaction occurs. Mathematically, entropy of the reaction is estimated from the experimentally obtained data that is positive (249.23 J mol^{-1} K^{-1}). So it can be explained that as temperature is increased above 333 K, desorption occurs on the Ca-SiO_2-TiO_2 surface, which results in the concentration of fluoride in solution being increased in small amount in solution.

Table 2. The Thomas model parameters at different conditions for the adsorption of fluoride

Flow rate (ml min^{-1})	k_{Th} (mL mg^{-1} min^{-1})	q_0 (mg g^{-1})	q_e, exp (mg g^{-1})	R^2
5.5	0.1376	65.451	65.987	0.979
8.5	0.1734	58.312	63.132	0.983
11.5	0.2086	55.863	61.472	0.985
Bed height				
2.5 cm	0.1471	59.114	62.445	0.971
4.5 cm	0.1923	61.323	64.975	0.979
6.5 cm	0.2198	65.087	67.528	0.973

4. Column Studies

To evaluate the effectiveness of Ca-SiO_2-TiO_2 for continuous model [27] fluoride adsorption, column experiments [28] were carried out. The effects of flow rate and bed height were investigated.

4-1. Effect of Feed Flow Rate

Flow rate plays an important role in evaluating the performance of de-fluoridation process. Therefore, the effect of flow rate on fluoride adsorption byCa-SiO_2-TiO_2 was studied in the range of flow rate between 5.5-11.5 mL min^{-1} and keeping the initial fluoride concentration and bed height unchanged. The effect of flow rate on breakthrough performance at the above operating conditions is depicted in Fig. 8. It is observed from the figure that the adsorption efficiency was higher at lower flow rate. This can be explained by the fact that at lower flow rate, the contact time of the fluoride ions is more, and as a result they get more time to capture the available reaction sites of the adsorbent. The fluoride ions also have more time to diffuse into the pores of the adsorbent through intra-particle diffusion. As the flow rate increases, the residence time of fluoride solution in the column decreases. The contact time of the fluoride ions with the adsorbent is very little and that's why they do not have enough time to capture the reaction sites on the adsorbent surface leaving the column before equilibrium occurs.

4-2. Effect of Bed Height

To find the effect of bed height on the breakthrough curve, the fluoride solution having concentration 50 mg L^{-1} was passed through

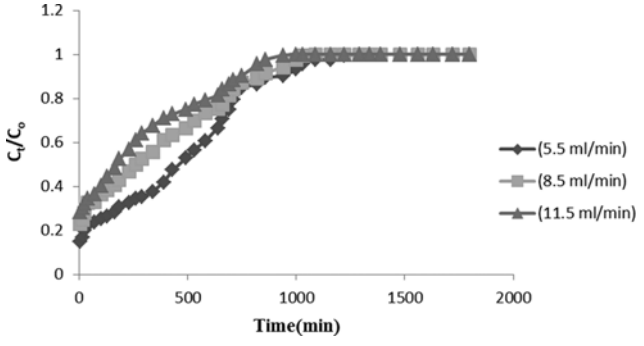

Fig. 8. Effect of flow rate on breakthrough curve for adsorptionof fluoride onto Ca-SiO_2-TiO_2 (Z=2.5 cm; C_0=50 mg L^{-1}).

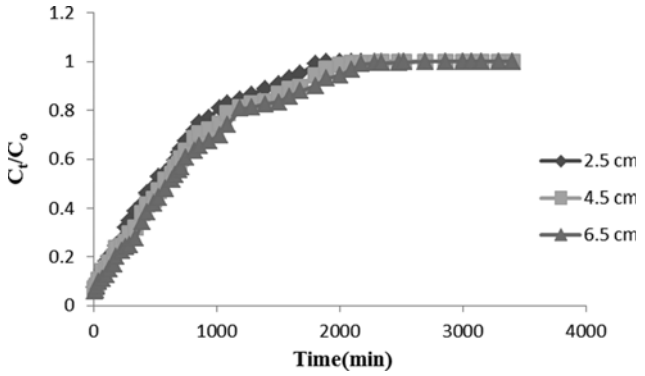

Fig. 9. Effect of bed height on breakthrough curve for adsorption of fluoride onto Ca-SiO_2-TiO_2 (u=5.5 ml min^{-1} cm; C_0=50 mg L^{-1}).

Table 3. The calculated constants of BDST model for the adsorption of fluoride (C_0=50 mg L^{-1}, u=5.5 ml min^{-1})

C_t/C_0	K_a (ml mg^{-1} min^{-1})	N_0 (mg L^{-1})	R^2
0.3	−209.1	187	0.99
0.6	−310.1	249	0.991
0.9	−338.7	298	0.999

the column at a flow rate of 5.5 mL min^{-1} by varying the bed height. Fig. 9 represents the performance of breakthrough curves at bed heights of 2.5 cm, 4.5 cm, and 6.5 cm. From Fig. 9 the breakthrough time increased with increasing bed depth from 2.5 to 6.5 cm. As the bed height increased, the fluoride molecules had more time to contact with the adsorbent, which resulted in higher removal efficiency of fluoride ions in the column. So a higher bed column results in decrease in the solute concentration in the effluent at the same time.

5. Modeling of Fixed Bed Column

5-1. Thomas Model

The Thomas rate constant (k_{Th}) and bed capacity (q_0) were calculated from the slope and intercept of the plot between $\ln(C_0/C_t-1)$ versus t at different flow rates and bed heights. The calculated values of k_{Th} and q_0 along with regression coefficients are presented in Table 3. The relatively high R^2 values at all the experimental conditions suggest that the Thomas model was suitable for describing the column adsorption data of fluoride by Ca-SiO_2-TiO_2. The calculated q_e values (q_0) show good agreement with the experimental q_e values (q_e, exp). It implies the good suitability of the Thomas model for column design and analysis. From Table 3, it is observed that as the flow rate increases, the bed capacity (q_0) decreases, while the Thomas rate constant (k_{Th}) increases. The Thomas model study is well fitted to the dynamic flow experimental data.

5-2. BDST Model

The BDST model basically measures the capacity of the bed at different breakthrough values. In this model the adsorbate is adsorbed onto the adsorbent surface directly (intraparticle mass transfer neglected). With these assumptions, the BDST model is well fitted to the modeling of column studies of de-fluoridation onto Ca-SiO_2-TiO_2.

The BDST model parameters K_a and N_0 are calculated, respectively, from the slope and intercept of the plot of t Vs Z at different experimental conditions, which are given in Table 4. The correlation coefficient (R^2) values are also given in Table 4. As the values of C_t/C_0 increased, the values of N_0 increased while K_a decreased The BDST model parameters can be useful for modeling with the dynamic flow experimental data.

Table 5. Central composite design (CCD) used for optimizing three independent variables along with the obtained response

Serial No.	A: Adsorbent dose (g)	B: Contact time (min)	C: Temperature (K)	R1 (%)
1	0.75	50	320.5	90.54
2	0.75	50	320.5	90.54
3	0.75	16.4	320.5	89.21
4	1	70	333	92.41
5	1.17	50	320.5	91.87
6	1	30	333	90.92
7	1	70	308	91.31
8	0.75	50	320.5	90.54
9	0.75	50	299.4	89.51
10	0.5	30	308	89.13
11	0.75	50	320.5	90.54
12	0.33	50	320.5	89.95
13	0.75	50	341.5	91.67
14	0.75	83.6	320.5	91.02
15	0.75	50	320.5	90.54
16	0.5	70	308	88.96
17	0.5	70	333	89.39
18	0.5	30	333	89.74
19	1	30	308	90.52
20	0.75	50	320.5	90.54

6. Estimation of Response Surface for Maximum Fluoride Removal

The results of the 20 experiments performed as per CCD analysis are shown in Table 5. The maximum fluoride removal was 92.41% at 70 min contact time, at 60 °C and 1.0 g of adsorbent. The

Table 4. Experimental range and levels of independent variables

Serial no.	Variable	Unit	Notation	Range and levels (coded)				
				$-\alpha$	−1	0	+1	$+\alpha$
(1)	Adsorbent dose	g	A	0.33	0.5	0.75	1.0	1.17
(2)	Contact time	min	B	16.4	30	50	70	83.6
(3)	Temperature	K	C	299.4	308	320.5	333	341.5

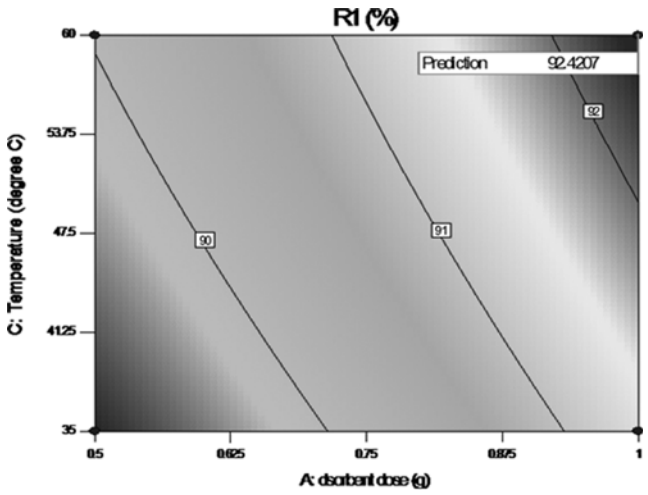

Fig. 10. RSM plot showing interaction effect of temperature and adsorbent dose.

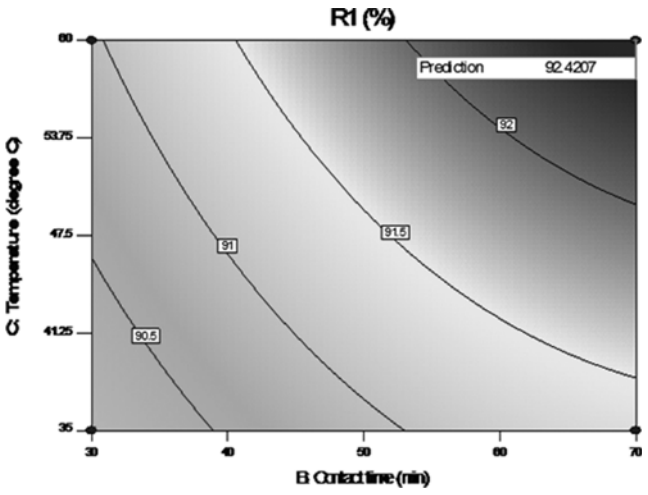

Fig. 11. RSM plot showing interaction effect of temperature and contact time.

response variable, which is expressed as a function of independent variables defined in quadratic model, developed by Design Expert software, is expressed in the form of different numerical factors in Eq. (14) given below:

$$\text{Removal \% of fluoride (R1)} = +90.55 + 0.081*A + 0.34*B + 0.44*C + 0.34*AB + 0.045*AC + 0.053*BC + 0.077*A^2 - 0.20*B^2 - 0.036\,C^2 \quad (14)$$

It is observed that A, B, C, AB, B^2, C^2 are significant model terms. The fitness of the model is verified by the correlation coefficient (R^2) between the experimental and model predicted values of the response variable. Statistically, R^2 value of 0.9893 indicates that the model is statistically significant. Therefore, the model is applied to predict the percentage removal of fluoride in solution within the limits of the experimental factors.

7. Interaction Effect of Process Variables

7-1. Effect of Variation in Adsorbent Dose and Temperature

The combined effect of adsorbent dose and temperature for adsorption on fluoride removal is illustrated in the contour plot of Fig. 10. It is found that percentage of fluoride removal increased on increasing the temperature from 300 K to 333 K and also increased in the range of adsorbent dose from 0.33-1.0 g. The higher values of fluoride removal may be obtained by increase in temperature and also with increase in adsorbent dose. Due to increase in adsorbent dosage, the electrostatic force of attraction between the fluoride ions and Ca-SiO_2-TiO_2 increased. From this given plot, maximum removal efficiency 92.41% is obtained at a 1.0 g adsorbent dose, at 333 K and 70 min of contact time.

7-2. Effect of Variation in Temperature and Contact Time

The effects of different temperature and reaction time are required to remediate fluoride in solution usingCa-SiO_2-TiO_2. It is proved from Fig. 11 that both the independent process variables play a significant role in the % fluoride adsorption process. From this contour plot, a maximal removal efficiency of 92.41% was achieved at 333 K and 1.0 g of Ca-SiO_2-TiO_2 while the other variable was set at the middle value. As the temperature increased from 300-333 K, the fluoride uptake capacity increased at particular adsorbent dose, which implies that the percentage of bound

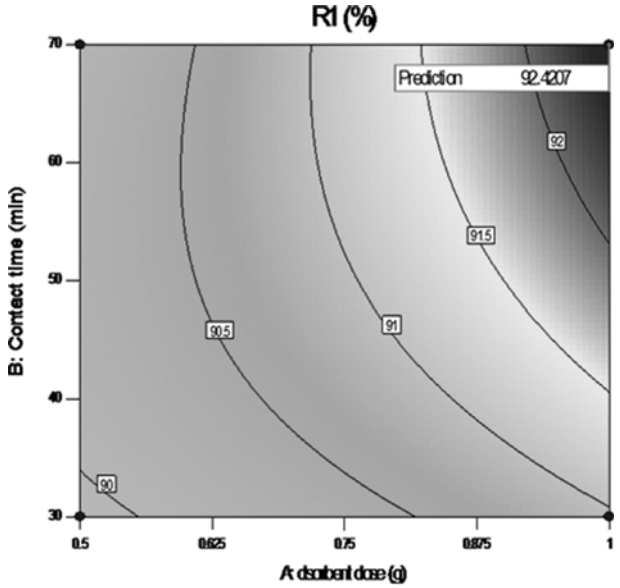

Fig. 12. RSM plot showing interaction effect of adsorbent dose and contact time.

fluoride ions adsorbed increases (due to higher attraction force between fluoride ions and Ca-SiO_2-TiO_2), consequently percentage efficiency of removal of fluoride ions increased.

7-3. Effect of Variation in Adsorbent Dose and Contact Time

The above plot of Fig. 12 depicts the interaction effects of the independent variables (contact time and adsorbent dose) in the above response. According to the contour plot of Fig. 12, de-fluoridation efficiency is increased with increasing dose of adsorbent and time of reaction. This trend is followed by maximum removal efficiency of 92.41%, obtained at 70 min contact time and adsorbent dose of 1.0 g.

8. Confirmational Study

The optimized data are supported by numerical modeling, which are verified by confirmatory experiments as suggested by the model (adsorbent dose 1.0 g; temperature 333 K; contact time 70 minutes).

Table 6. Comparative study of adsorption capacity, and isotherm model of various adsorbents with Ca-SiO_2-TiO_2 synthesized in this study

Name of sorbent	Maximum adsorption capacity	Isotherm	Reference
Glutaraldehyde Crosslinked Calcium Alginate	73.5 $mg \cdot g^{-1}$	Langmuir	[29]
Chitosan Coated Silica	44.4 $mg \cdot g^{-1}$	Langmuir, Freundlich	[30]
Chitosan based mesoporous Ti-Al binary metal oxide	2.22 $mg \cdot g^{-1}$	Langmuir	[31]
Zirconium(IV)-impregnated collagen fiber	2.18 $mmol \cdot g^{-1}$	Langmuir	[32]
Aluminum modified zeolitic tuff	10.25 $mg \cdot g^{-1}$	Langmuir-Freundlich	[33]
Alginate entrapped Fe(III)-Zr(IV) binary mixed oxide	0.981 $mg \cdot g^{-1}$	Langmuir	[34]
Calcium chloride modified natural zeolite	1.766 $mg \cdot g^{-1}$	Langmuir	[35]
Fe-Al-Ce hydroxide	51.3 $mg \cdot g^{-1}$	Langmuir	[36]
Fe-Ti oxide nano-adsorbent	47 $mg \cdot g^{-1}$	Langmuir	[37]
Nitrate containing ZnCr layered double hydroxides	31 $mg \cdot g^{-1}$	Langmuir	[38]
Zirconium phosphate	4.268 $mg \cdot g^{-1}$	Langmuir	[39]
Calcium impregnated silica combined with TiO_2 (Ca-SiO_2-TiO_2)	37.23 $mg \cdot g^{-1}$	Langmuir	Present study

These are found to be optimum conditions for maximum percent fluoride removal, and in that condition the maximum fluoride removal obtained as 92.41% and experimentally it is 92.46%. The difference between the removal efficiency in the two conditions is 0.05%.

CONCLUSION

Our goal was to study the defluoridation process onto Ca-SiO_2-TiO_2 to investigate the influence of various process parameters on fluoride removal using batch isotherm, kinetics study and response surface methodology. The adsorption studies were carried out as a function of temperature, contact time, adsorbent dose. The defluoridation efficiency was majorly affected by reaction temperature, contact time, adsorbent dose. The levels of the three variables such as temperature 333 K, contact time 70 min, adsorbent dose 1.0 g were found to be optimum for maximum defluoridation. The corresponding percentage of defluoridation in optimum conditions was found to be 92.41%. The experimental results are well fitted to the Langmuir isotherm model and follow pseudo-second-order kinetic model. In the fixed-bed adsorption studies, the breakthrough curves are affected by both flow rate and bed-height. A comparative study of these adsorbents with various other adsorbents used for defluoridation has been provided (Table 6), which elucidates the efficacy of these adsorbents. As silica, calcium chloride and titanium dioxide are easily available, so the chemical synthesis Ca-SiO_2-TiO_2 of is not so difficult a process. Hence, it may serve as an effective adsorbent for removal of fluoride ion from solution.

ACKNOWLEDGEMENTS

This study was supported by Department of Chemical Engineering, Jadavpur University, India and West Bengal Pollution Control Board, India. Authors are thankful for their support and service.

NOMENCLATURE

A : Arrhenius constant
C_a : equilibrium fluoride concentration on the adsorbent [$mg\ L^{-1}$]
C_e : equilibrium fluoride concentration in solution [$mg\ L^{-1}$]
C_i : initial fluoride concentration [$mg\ L^{-1}$]
C_o : influent fluoride concentration [$mg\ L^{-1}$]
C_t : effluent fluoride concentration [$mg\ L^{-1}$]
E_a : activation energy [$kJ\ mol^{-1}$]
ΔG^0 : Gibbs free energy change [$kJ\ mol^{-1}$]
ΔH^0 : Enthalpy of reaction [$kJ\ mol^{-1}$]
ΔS^0 : Entropy of reaction
z : bed height [cm]
K_c : distribution coefficient for adsorption
K_F : Freundlich constant [$mg\ g^{-1}$] [$L\ g^{-1}$]1/n
K_L : Langmuir constant [$L\ mg^{-1}$]
k : rate constant
k_1 : pseudo-first-order rate constant [min^{-1}]
k_2 : pseudo-second-order rate constant [$g\ mg^{-1}\ min^{-1}$]
m : mass of adsorbent [g]
n : Freundlich adsorption isotherm constant
q_e : equilibrium fluoride concentration on adsorbent [$mg\ g^{-1}$]
q_m : maximum adsorption capacity [$mg\ g^{-1}$]
q_t : amount of fluoride adsorbed at time t [$mg\ g^{-1}$]

REFERENCES

1. M. G. Sujana, H. K. Pradhan and S. Anand, *J. Hazard. Mater.*, **161**, 120 (2009).
2. WHO, Guidelines for Drinking Water Quality, 3rd Ed., Geneva (2004).
3. N. J. Chinoy, *Indian J. Environ. Toxicol.*, **1**, 17 (1991).
4. N. Chen, Z. Zhang, C. Feng, M. Li, D. Zhu and N. Sugiura, *Mater. Chem. Phys.*, **125**, 293 (2011).
5. N. Das, P. Pattanaik and R. Das, *J. Colloid Interface Sci.*, **292**, 1 (2005).

6. S. S. Tripathy, J. L. Bersillon and K. Gopal, *Sep. Purif. Technol.*, **50**, 310 (2006).
7. L. M. Camacho, A. Torres, D. Saha and S. Deng, *J. Colloid Interface Science*, **349**, 307 (2010).
8. D. Mohan, K. P. Singh and V. K. Singh, *J. Hazard. Mater.*, **152**, 1045 (2008).
9. G. Alagumuthu and M. Rajan, *Hem. Ind.*, **64**, 295 (2010).
10. G. Alagumuthu, V. Veeraputhiran and R. Venkataraman, *Hem. Ind.*, **65**, 23 (2011).
11. Y. LiuZheng and A. Wang, *Ads. Sci. Technol.*, **28**(10), 913 (2010).
12. M. Mourabet, A. El. Rhilassi, H. El. Boujaady, M. Bennani-Ziatni, R. El. Hamri and A. Taitai, *Appl. Water Sci.*, **258**, 4402 (2012).
13. V. Hernández-Montoyaa, L. A. Ramírez-Montoya, A. Bonilla-Petriciolet and M. A. Montes-Moránb, *Biochem. Eng. J.*, **62**, 1 (2012).
14. D. Bas and I. H. Boyaci, *J. Food Eng.*, **78**, 836 (2007).
15. M. A. Bezerra, R. E. Santelli, E. P. Oliveira, L. S. Villar and L. A. Escaleira, *Talanta*, **76**, 965 (2008).
16. I. Arslan-Alaton, G. Tureliamd and T. Olmez-Hanci, *J. Photochem. Photobiol. A*, **202**, 142 (2009).
17. K. Thirugnanasambandham, V. Sivakumar, J. Prakash Maran and S. Kandasamy, *J. Korean Chem. Soc.*, **57**, 761 (2013).
18. M. Mohapatra, S. Anand, B. K. Mishra, D. E. Giles and P. Singh, *J. Environ. Manage.*, **91**, 67 (2009).
19. Bhatnagar, E. Kumar and M. Sillanpää, *Chem. Eng. J.*, **171**, 811 (2011).
20. A. Dąbrowski, *Adv. Colloid Interface Sci.*, **93**, 135 (2001).
21. H. Žabova, J. Sobek, V. Církva, O. Šolcova and M. Hájek, *J. Solid State Chem.*, **182**(12), 3387 (2009).
22. I. Langmuir, *J. Am. Chem. Soc.*, **40**, 1361 (1918).
23. H. Freundlich, *Z. Phys. Chem.*, **57**, 384 (1906).
24. F. Rozada, M. Otero, A. I. Garcia and A. Moran, *Dyes Pigm.*, **72**, 47 (2007).
25. M. Jain, V. K. Garg and K. Kadrivelu, *Bioresour. Technol.*, **102**, 600 (2011).
26. M. Amini, H. Younesi, N. Bahramifar, A. A. A. Lorestani, F. Ghorbani, A. Daneshi and M. Sharifzadeh, *J. Hazard. Mater.*, **54**, 694 (2008).
27. T. W. Webi and R. K. Chakravort, *AIChE J.*, **20**, 228 (1974).
28. S. Ghorai and K. K. Pant, *Sep. Purif. Technol.*, **42**, 265 (2005).
29. Y. Vijaya, S. R. Popuri, A. S. Reddy and A. Krishnaiah, *J. Appl. Polym. Sci.*, **120**, 3443 (2011).
30. Y. Vijaya and A. Krishnaiah, *E-J. Chem.*, **6**, 713 (2009).
31. D. Thakre, S. Jagtap, N. Sakhare, N. Labhsetwar, S. Meshram and S. Rayalu, *Chem. Eng. J.*, **158**, 315 (2010).
32. X. P. Liao and B. Shi, *Environ. Sci. Technol.*, **39**, 4628 (2005).
33. A. Teutli-Sequeira, M. Solache-Ríos, V. Martínez-Miranda and I. Linares-Hernández, *J. Colloid Interface Sci.*, **418**, 254 (2014).
34. S. K. Swain, T. Patnaik, P. C. Patnaik, U. Jha and R. K. Dey, *Chem. Eng. J.*, **215-216**, 763 (2013).
35. Z. Zhang, Y. Tan and M. Zhong, *Desalination*, **276**, 246 (2011).
36. B. Zhao, Y. Zhang, X. Dou, X. Wu and M. Yang, *Chem. Eng. J.*, **185-186**, 211 (2012).
37. K. Babaeivelni and A. P. Khodadoust, *J. Colloid Interface Sci.*, **394**, 419 (2013).
38. P. Koilraj and S. Kannan, *Chem. Eng. J.*, **234**, 406 (2013).
39. S. K. Swain, T. Patnaik, V. K. Singha, U. Jha, R. K. Patel and R. K. Dey, *Chem. Eng. J.*, **171**, 1218 (2011).